Current Applied Physics

4.3
CiteScore

2.480
Impact Factor

About the journal

Editor-in-Chief

Bongjin Simon Mun
Gwangju Institute of Science and Technology, Gwangju, South Korea
Email this editor

Executive Editor

Jae-Won Jang
Dongguk University Department of Semiconductor Science, Seoul, South Korea
Email this editor

Vice Executive Editors

Sunghwan Kim
Ajou University, Suwon, South Korea
Email this editor

Geun Woo Lee

Korea Research Institute of Standards and Science, Daejeon, South Korea
Email this editor

Editorial Board

Dong-Hyun Kim
Chungbuk National University, Cheongju, South Korea

Hyun You Kim
Chungnam National University, Daejeon, South Korea

Jun Sung Kim
Pohang University of Science and Technology, Pohang, The Republic of Korea Center for Artistic Low Dimensional Electronic Systems, Institute for Basic Science, South Korea

Kwanpyo Kim
Yonsei University, Seoul, South Korea

Myung Hwa Kim
Ewha Womans University, Seoul, South Korea

Sanghoon Kim
University of Ulsan, Ulsan, South Korea

Sooran Kim
Kangwon National University Department of Physics, Daegu, South Korea

Yunseok Kim
Sungkyunkwan University, Suwon, South Korea

Changhyun Ko
Sookmyung Women's University, Yongsan-gu, South Korea

Dong Su Lee
Korea Institute of Science and Technology, Seongbuk-gu, South Korea

Dongwoo Lee
Sungkyunkwan University College of Engineering, Suwon, South Korea

Hyun Seok Lee
Chungbuk National University, Cheongju, South Korea

Hyunbok Lee
Kangwon National University, Chuncheon, South Korea

Sang-Kwon Lee
Chung-Ang University, Seoul, South Korea

International Advisory Editorial Board

Esther Conwell
University of Rochester, Rochester, New York, NY, USA

Lev Gor'kov
Florida State University, Tallahassee, FL, United States of America

Alan Heeger
University of California Santa Barbara Department of Physics, Santa Barbara, California, United States of America

Denis Jérome
Paris-Saclay University, St Aubin, France

Yung Woo Park
Seoul National University, Seoul, South Korea

George Sawatzky
The University of British Columbia, Vancouver, British Columbia, Canada

John Robert Schrieffer
Florida State University, Tallahassee, FL, United States of America

Hideki. Shirakawa
University of Tsukuba, Tsukuba, Japan

Frans Spaepen
Harvard University, Cambridge, MA, United States of America

Ken Suzuki
Tohoku University, Miyagi, Japan

Masashi Tachiki
National Institute for Materials Science, Tsukuba-Shi, Japan

Shoji Tanaka
International Superconductivity Technology Center Superconductivity Research Laboratory, Koto-Ku, Japan

Fosong Wang
Chinese Academy of Sciences, Beijing, China

Chung Nam Whang

Publisher

The Korean Physical Society
The Korean Science Technology Center (Rm.601), 22, Teheran-ro 7-gil, Gangnam-gu, 06130, Seoul, Republic of Korea

Contact Information

In-Ji Song

All members of the Editorial Board have identified their affiliated institutions or organizations, along with the corresponding country or geographic region. Elsevier remains neutral with regard to any jurisdictional claims.

ISSN: 1567-1739

Current Applied Physics 20 (2020) 638–642

Contents lists available at ScienceDirect

Current Applied Physics

journal homepage: www.elsevier.com/locate/cap

Bio-silica incorporated barium ferrite composites: Evaluation of structure, morphology, magnetic and microwave absorption traits

Wahyu Widanarto[a,*], Mukhtar Effendi[a], Sib Krishna Ghoshal[b], Candra Kurniawan[c], Erfan Handoko[d], Mudrik Alaydrus[e]

[a] Department of Physics, FMIPA, Universitas Jenderal Soedirman, Jl. dr. Soeparno 61, Purwokerto, 53123, Indonesia
[b] Department of Physics and Laser Centre, AMORG, Faculty of Science, Universiti Teknologi Malaysia, Johor Bahru, Skudai, 81310, Malaysia
[c] Research Center for Physics, Indonesian Institute of Sciences (LIPI), Puspiptek Office Area, South Tangerang, Banten, 15314, Indonesia
[d] Department of Physics, Universitas Negeri Jakarta, Jl. Rawamangun Muka, Jakarta, 13220, Indonesia
[e] Department of Electrical Engineering, Universitas Mercu Buana, Jl. Meruya Selatan, Jakarta, 11650, Indonesia

ARTICLE INFO

Keywords:
Bio-silica
Barium ferrite
Magnetic properties
Permittivity
Permeability
Reflection loss

ABSTRACT

A series of bio-silica incorporated barium-ferrite-composites with the composition of (x)Bio-SiO_2:$(80\text{-}x)\gamma$-Fe_2O_3:(20)BaO, where x = 0, 1, 2, and 3 wt% were prepared using the modified solid-state reaction method. The influence of different bio-silica (extricated from sintered rice husk) contents on the surface morphologies, structures, and magnetic characteristics of these composites were assessed. The relative complex permittivity and permeability were resolved using the Nicholson-Ross-Weir strategy in the frequency range of 8–13 GHz. Meanwhile, the reflection loss was estimated through the transmission/reflection line theory to assess the MW absorption properties of the composites. Incorporation of the bio-silica in the barium ferrite composites generated a new hexagonal phase ($Ba_3Fe_{32}O_{51}$) and a tetragonal phase ($BaFeSi_4O_{10}$) which led to a decrease in the saturation magnetization and significant shift in the MW frequency absorption peak positions.

1. Introduction

In recent times, microwave (MW) absorbing materials became one of the key high-tech candidates for the development of the high-performance device in the field of anti-radar technology, wireless communications, and shielding of electromagnetic wave interferences [1–3]. The coating of the targets with MW absorbing materials emerged as a strategy to reduce the intensity of the reflected electromagnetic waves. This technique utilizes the absorption or dispersion of electromagnetic energy in the material medium between the electromagnetic wave source and the protected target. For such purposes, materials must be fit for weakening and dispersing the overabundance measure of the electromagnetic radiation in the form of heat through the mechanisms of magnetic and dielectric loss [4]. Likewise, innovative magnetic materials, particularly ferrites based, are uncovered to be suitable for absorbing the MW and have frequently been investigated [5–13].

It has been verified that a barium ferrite system (a magnetic material) with a wide crystalline anisotropic magnetic field can potentially be used in the GHz frequency range compared to other ferrites with spinel and garnet structures [2,14]. Thus, the barium hexaferrite (BHF) owing to their unusual strong uniaxial anisotropic magnetic field was prepared as MW absorbing material [6–8,15,16]. The literature reports revealed that the replacement of Fe^{3+} by trivalent lanthanide ions (used as doping agent) is an effective way to shift the resonant frequency (f_r) and change the anisotropy field (H_A), influencing the MW absorption capacity of the magnetic material [2,9,17–21]. However, the scarcity and high prices of rare earth materials limit their widespread usages. Thus, the exploration of the doping agent alternative to the rare-earth ions (acts as an activator) became mandatory to fulfill such need.

Categorically, silica is a famous semiconducting material that can be obtained either commercially or from plentiful natural resources. Interestingly, rice husk after complete combustion can be a great source of bio-silica. Such bio-silica derived from rice husk (as abundant raw material) has several advantages compared to silica minerals, including the existence of fine grain, high reactivity, low cost and can function as a heavy metal binder. Encouraged by these notable benefits of rice husk extracted bio-silica, we prepared some bio-silica integrated barium ferrite composites (hereafter called SiBFCs) to reduce the values of coercive field (H_c) and saturation magnetization (M_s), in that way enhancement of the selective MW absorption capacity of the achieved SiBFCs.

* Corresponding author.
E-mail address: wahyu.widanarto@unsoed.ac.id (W. Widanarto).

https://doi.org/10.1016/j.cap.2020.02.019
Received 27 October 2019; Received in revised form 22 February 2020; Accepted 24 February 2020
Available online 26 February 2020

This paper reports the synthesis and characterizations of the newly prepared SiBFCs, wherein the bio-silica at various concentrations were merged in pure barium hexaferrite. The undoped and doped composites were prepared via a solid−state reaction method. These as-prepared SiBFCs were characterized using diverse analytical apparatuses to assess the effects of various bio-silica contents on the microstructure, morphology, magnetic properties, and MW reflection losses in the frequency range of GHz. The obtained $BaFeSi_4O_{10}$ and $Ba_3Fe_{32}O_{51}$ composites were given away to be valuable for several applications.

2. Experimental procedures

Four samples of SiBFCs with the composition of (x)Bio-SiO_2:(80-x)γ-Fe_2O_3:(20)BaO, (x = 0, 1, 2 and 3 in wt%) were synthesised via the modified solid-state reaction method. Highly pure powders of $BaCO_3$ (from Merck with the purity of 99%), bio-silica, and γ-Fe_2O_3 as primary raw constituents were utilized to prepare these SiBFCs. The $BaCO_3$ powder was calcined at 350 °C for 15 min in the air atmosphere to eliminate the presence of the carbon component. The bio-silica was obtained by sintering the rice husk ash at a temperature of 1000 °C for 3 h in the air atmosphere. Meanwhile, the Fe_3O_4 was extracted from the iron sand [22] and sintered at 850 °C in the air atmosphere for 3 h to obtain γ-Fe_2O_3. Afterward, the bio-silica powder was mixed gradually with the γ-Fe_2O_3 and BaO powder. The mixed constituent powder was compressed to yield the pellet of 1 mm thick and 10 mm diameter [19]. Additionally, all the pellets were strengthened and sintered at 800 °C (for 1 h) and 1100 °C (for 5 h) an air atmosphere before they were cooled down to the room temperature naturally. The acquired pellets were named as SiBF0, SiBF1, SiBF2, and SiBF3, depending on the matching bio-silica content of 0, 1, 2, and 3 wt%. For further characterizations, some pellets were crushed. Finally, the crushed pellets were mixed with epoxy resin at a mass ratio of 7:3 to get a rectangular-shaped sample of dimension (2.3 cm × 1.0 cm × 0.5 cm) using a WR90 sample holder.

The surface morphology and microstructure of the prepared SiBFCs were characterized using the scanning electron microscope (SEM, Hitachi SU 3500). The crystalline nature of the prepared SiBFCs was confirmed using the X-ray diffraction (XRD, SmartLab 3 kW) furnished with Cu−Kα radiation of wavelength (λ) ≈ 0.1541874 nm. The vibrating sample magnetometer (VSM, Oxford 1.2H) was used to scrutinize the magnetic traits of the proposed samples. The scattering parameters (S) of the samples were recorded on a vector network analyzer (VNA, Keysight PNA-L N5232A) operated in the frequency range of 8–13 GHz. The MW absorption measurement was conducted to yield the scattering parameters such as S_{11}, S_{12}, S_{21}, and S_{22} (S-parameters). The value of S_{11} (= S_{22}) signified the reflection coefficient (Γ) and S_{21} (= S_{12}) represented the transmission coefficient (T). The values of complex relative permeability (μ_r) and permittivity (ε_r) were obtained following the Nicholson-Ross-Weir (NRW) relations given by:

$$\mu_r = \frac{1+\Gamma}{\Lambda(1-\Gamma)\sqrt{\frac{1}{\lambda_0^2}-\frac{1}{\lambda_c^2}}} \quad (1)$$

$$\frac{1}{\Lambda^2} = -\left[\frac{1}{2\pi d}\ln\left(\frac{1}{T}\right)\right]^2 \quad (2)$$

$$\varepsilon_r = \frac{\lambda_0^2}{\mu_r}\left(\frac{1}{\lambda_c^2} - \left[\frac{1}{2\pi d}\ln\left(\frac{1}{T}\right)\right]^2\right) \quad (3)$$

where λ_0 is the wavelength in vacuum, λ_c is the cut-off wavelength, c is the speed of the light, and d is the thickness of the sample.

3. Results and discussions

Fig. 1 depicts the XRD pattern of the synthesized bio-silica, confirming all the diffraction peaks due to the tetragonal crystal system of

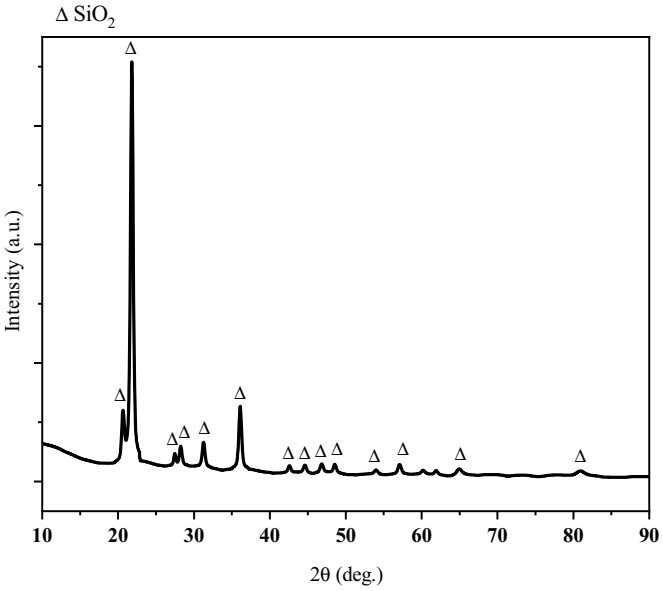

Fig. 1. The XRD pattern of the bio-silica (SiO_2) at 1000 °C.

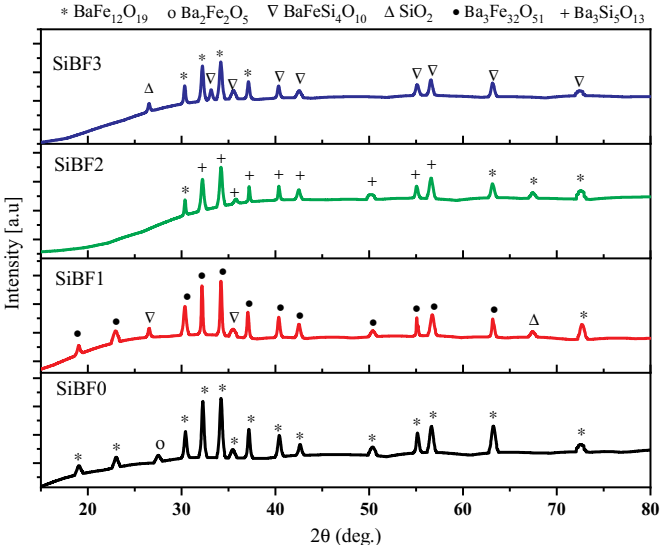

Fig. 2. The XRD patterns of the Si^{4+} undoped and doped SiBFCs.

SiO_2. Fig. 2 displays the XRD diffractograms of the produced SiBFCs that consisted of many characteristic peaks assigned to altering crystalline lattices. All the observed peaks in the pristine sample (SiBF0 without bio-silica incorporation) were due to the main hexagonal crystalline lattice of $BaFe_{12}O_{19}$ and tallied to the ICDD card number 00-039-1433 with crystal configurations of $a = b = 0.5894$ nm, $c = 2.3215$ nm, $\alpha = \beta = 90°$ and $\gamma = 120°$. Nevertheless, the appeared peak at 27.52° was due to the monoclinic crystalline phase of $Ba_2Fe_2O_5$ that corresponded to the ICDD card number 00-043-0256. The XRD pattern of SiBF1 sample revealed that the replacement of Fe^{3+} in the barium ferrite lattice by Si^{4+} ions at one wt% of SiO_2 did not cause any significant changes of the crystal structures. The appearance of two dominant peaks in SiBF1 confirmed the formation of the major phase of $Ba_3Fe_{32}O_{51}$ and minor phase of barium iron silicate $BaFeSi_4O_{10}$. The occurrences of sharp XRD peaks were due to the hexagonal crystal lattice of $Ba_3Fe_{32}O_{51}$ that corresponded to the ICDD card number 00-041-0846 with the crystal configurations of $a = b = 0.5892$ nm, $c = 2.3198$ nm, $\alpha = \beta = 90°$ and $\gamma = 120°$. Moreover, the peaks centered at 26.52° and 35.48° were assigned to the tetragonal crystal

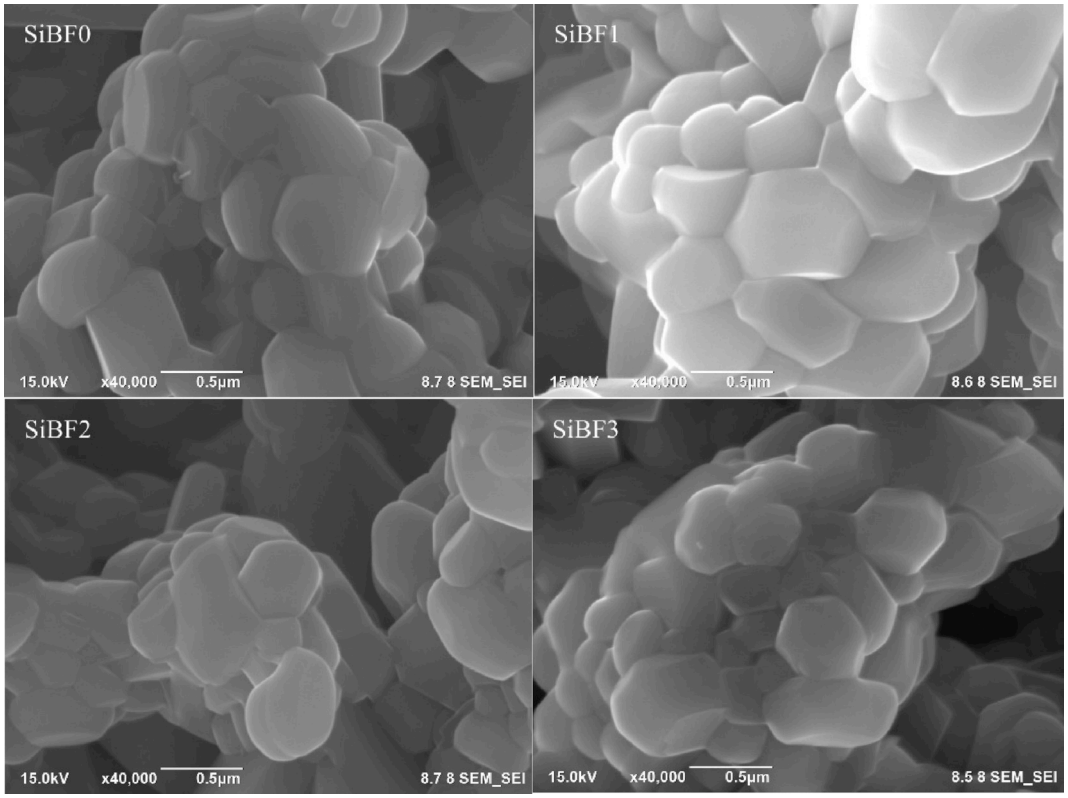

Fig. 3. The SEM images of the SiBFCs.

lattice planer orientation of $BaFeSi_4O_{10}$ (tallied to the ICDD card number 00-003-0402). The XRD pattern of the composite prepared with two wt% of bio-silica revealed a new phase of barium silicate $Ba_3Si_5O_{13}$ with the monoclinic crystalline lattice structure (agreed to the ICDD number 00-026-0179). The composite containing three wt% of bio-silica exhibited the dominant barium iron silicate $BaFeSi_4O_{10}$ ordered phase. It was claimed that the replacement of Fe^{3+} ions by Si^{4+} in the produced BFCs could create another significant hexagonal phase of $Ba_3Fe_{32}O_{51}$ and a tetragonal phase of $BaFeSi_4O_{10}$. The observed broadening in the XRD peaks for all the studied SiBFCs is attributed to the insolvent of lattice strain and nano-crystallites size confinement effects [23,24].

Fig. 3 shows the SEM micrographs of the prepared SiBFCs, which consisted of hexagonal particle morphology (particle size of about 0.5 μm) with irregular microstructures packing. These porous composite particles were attached to each other and formed some intergranular pores. It can be argued that the substitution of the Fe^{3+} by Si^{4+} (from the bio-silica) in the produced BFCs that created a new tetragonal phase of $BaFeSi_4O_{10}$ were closely packed to the hexagonal phase of $Ba_3Fe_{32}O_{51}$. In the intergranular pores of these composite particles phase, the Si^{4+} were preferentially occupied in the lattice sites, imparting more porosity to the microstructures. These pores, in turn, favored the entrapment of the MW, wherein the finer particles present in the pores could scatter the MW randomly in all directions, thereby modifying the MW absorption characteristics of the composites. In all the prepared SiBFCs, these distinct types of surface morphologies and particle distribution were responsible for the changes in the magnetic and reflection loss properties.

Fig. 4 represents the room temperature hysteresis loops (*M-H* curves) of the as-synthesized SiBFCs. The values of saturation magnetization of the studied SiBFCs are decreased (from 39.5 to 30.4 emu/g) significantly with the addition of bio-silica (from 1 to 3 wt%) into the composites. However, the coercive field values (altered from 775.9 to 811.0 Oe) are not affected appreciably due to the increase in bio-silica

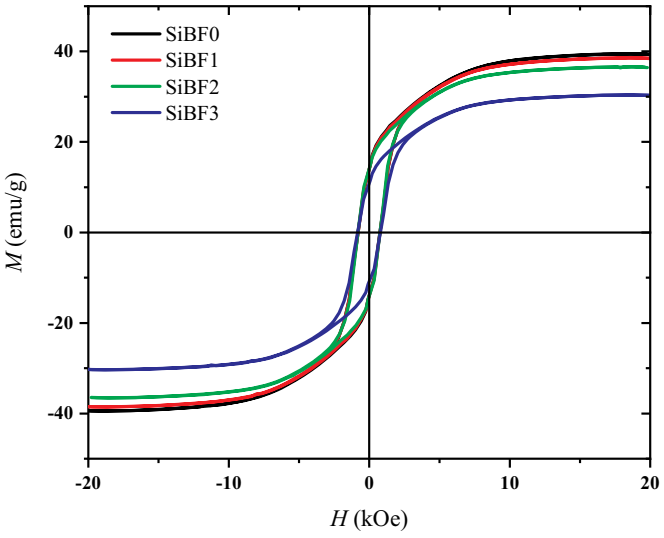

Fig. 4. The room temperature hysteresis loops (*M-H*) of the SiBFCs.

contents. The maximum reduction in the saturation magnetization displayed by the SiBF3 sample is ascribed to the presence of dominant tetragonal barium iron silicate ($BaFeSi_4O_{10}$) crystalline phase in the composite. The coercive field values of the composites are observed to increase slightly due to the rise in bio-silica contents. With the increase in bio-silica content from 0 to 2 wt%, the area of the hysteresis loop of the SiBFCs enlarges from 15.9 to 31.0 kOe.emu/g, respectively. Furthermore, the hysteresis loop area of SiBFC shrinks at three wt% of bio-silica. The observed change in the magnetic permeability of SiBFCs with the addition of bio-silica into the composites is majorly attributed to the alteration in the saturation magnetization and coercive field values.

Fig. 5(a) illustrates the frequency-dependent complex relative

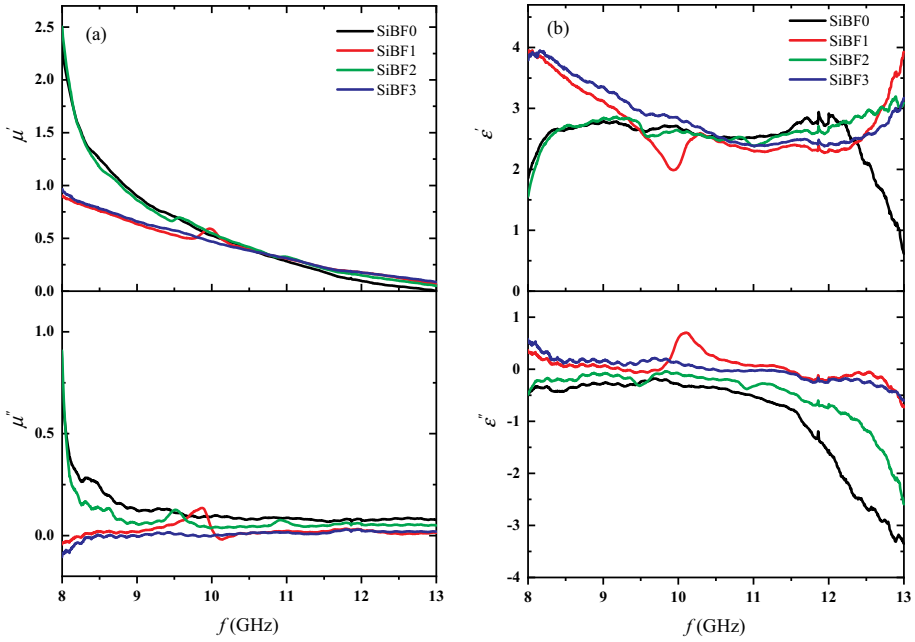

Fig. 5. Frequency-dependent complex relative (a) permeability and (b) permittivity of the SiBFCs with a thickness of 0.5 cm.

permeability ($\mu_r = \mu' + \mu''$) of all the SiBFCs. The real part of the permeability (μ') specifies a gradual decrease in their magnetic energy storing capacity due to polarization of magnetic dipole in higher MW frequency. The μ' value of the composites drops from about 2.5 (for SiBF0 and SiBF2) and 0.9 (for SiBF1 and SiBF3) to near-zero with the increase in bio-silica content from 0 to 3 wt%. Meanwhile, the observed magnetic loss is revealed by the imaginary part of the permeability (μ''). The μ'' value of SiBF0 and SiBF2 declines rapidly from 0.9 to near-zero and almost remains constant near-zero for SiBF1 and SiBF3 due to the relaxation process, which generates dissipation energy of MV as thermal energy.

Fig. 5(b) displays the complex relative permittivity ($\varepsilon_r = \varepsilon' + \varepsilon''$) of all the SiBFCs in the frequency range of 8–13 GHz. The ε' and ε'' are the real and imaginary parts of the permittivity, respectively. The ε' value indicated the lack of energy absorption by the composite from an externally applied electric field [25]. The ε' values of the composite without bio-silica doping (SiBF0) were dropped sharply. Conversely, the ε' values of the composites containing bio-silica (1–3 wt%) were increased significantly above 12 GHz due to the electrical dipole polarization. The value of ε'' (called the dielectric loss factor) denotes the electrical energy dissipation ability of the SiBFCs. The ε'' values of all SiBFCs were decreased gradually with the rise in the frequency.

The MW absorption properties of SiBFCs were evaluated by calculating the values of reflection loss (R_L) based on the transmission/reflection line theory [26–28]:

$$R_L = -20 \log \left| \frac{Z_{in} - Z_0}{Z_{in} + Z_0} \right| \tag{4}$$

$$Z_{in} = Z_0 \sqrt{\frac{\mu_r}{\varepsilon_r}} \tanh \left[j \frac{2\pi f d}{c} \sqrt{\mu_r \varepsilon_r} \right] \tag{5}$$

where Z_0 and Z_{in} are the corresponding intrinsic impedance in a vacuum and the input impedance in the material, f represents the MW frequency, d denotes the sample thickness, and c is the light speed in the vacuum.

Fig. 6 illustrates the frequency-dependent changes in the R_L values of the prepared SiBFCs. The MW absorption ability of materials is determined by two crucial factors i.e. R_L and bandwidth. The value of R_L for SiBF0 was valued less than −10 dB at the frequency of 8.35, 9.37, and 10.60 GHz. The band positions (peak frequencies) of the

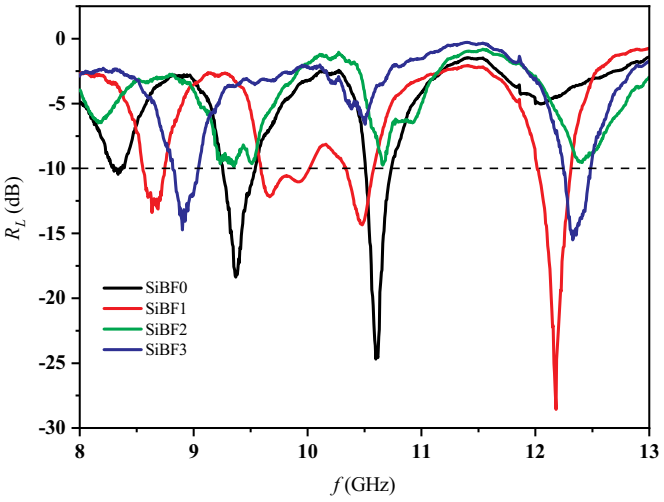

Fig. 6. Reflection loss as a function of the MW frequency for the studied SiBFCs of 0.5 cm thick.

composites disclose a significant shift with the change in bio-silica contents with the bandwidth of less than 1 GHz. The sample prepared with one wt% of bio-silica (SiBF1) reveals the lowest R_L value of −28.56 dB at the frequency of 12.18 GHz. This disclosure affirms that the MW absorption capacity of the proposed SiBFCs can be essentially customized by controlling the impurity or dopant (bio-silica) concentration, fulfilling the application demand in the X band. Some strategies were employed to modify the dielectric and magnetic parameters including the single trivalent cation substitution and different combinations of cation to minimize the MW reflection loss [27,29]. Compared to the earlier materials, present bio-silica based composites are cheaper and easy to prepare.

4. Conclusions

Considering the MW absorption potency of barium ferrites, we synthesized four SiBFCs (without and with bio-silica activation) via the modified solid-state reaction approach. Rice husk derived abundant and cheap bio-silica was doped into the barium ferrites to improve their

magnetic and MW absorption attributes. The structure of the studied composites revealed the presence of various crystalline phases. The surface of SiBFCs disclosed hexagonal morphology with a particle size of about 0.5 μm. The surface morphology, structure, MW reflection loss, permittivity, permeability, coercivity, saturation magnetization, and MW absorption of the proposed SiBFCs were found to be sensitive to the substitution of Fe^{3+} by Si^{4+} ions into the composite matrix. It was established that the MW absorption ability of the newly composed SiBFCs can be tailored by adjusting the bio-silica content. Present knowledge may contribute towards the development of the SiBFCs based MW absorption devices.

Declaration of competing interest

No conflict of interest exists.

Acknowledgments

The authors appreciated the financial support from the Universitas Jenderal Soedirman, Kemenristekdikti Indonesia, and UTM Malaysia (MOHE, FRGS/KPT 5F050 and GUP 20H65).

References

[1] H. Zhao, G. Zhang, R. Ma, Synthesis and electromagnetic properties of nanocrystalline Ni-Zn Ferrite doped lanthanum, Nanotechnol. Precis. Eng. 8 (2010).
[2] C.-J. Li, B. Wang, J.-N. Wang, Magnetic and microwave absorbing properties of electrospun $Ba_{(1-x)}La_xFe_{12}O_{19}$ nanofibers, J. Magn. Magn Mater. 324 (2012) 1305–1311, https://doi.org/10.1016/j.jmmm.2011.11.016.
[3] B.K. Rai, S.R. Mishra, V.V. Nguyen, J.P. Liu, Synthesis and characterization of high coercivity rare-earth ion doped $Sr_{0.9}RE_{0.1}Fe_{10}Al_2O_{19}$ (RE: Y, La, Ce, Pr, Nd, Sm, and Gd), J. Alloys Compd. 550 (2013) 198–203, https://doi.org/10.1016/j.jallcom.2012.09.021.
[4] M.S. Kim, J.G. Koh, Microwave-absorbing characteristics of NiCoZn ferrite prepared by using a co-precipitation method, J. Kor. Phys. Soc. 53 (2008) 737–741.
[5] C.L. Yuan, Y.S. Tuo, Microwave adsorption of $Sr(MnTi)_xFe_{12-2x}O_{19}$ particles, J. Magn. Magn Mater. 342 (2013) 47–53, https://doi.org/10.1016/j.jmmm.2013.04.038.
[6] C. Sun, K. Sun, P. Chui, Microwave absorption properties of Ce-substituted M-type barium ferrite, J. Magn. Magn Mater. 324 (2012) 802–805, https://doi.org/10.1016/j.jmmm.2011.09.023.
[7] C. Dong, X. Wang, P. Zhou, T. Liu, J. Xie, L. Deng, Microwave magnetic and absorption properties of M-type ferrite $BaCo_xTi_xFe_{12-2x}O_{19}$ in the Ka band, J. Magn. Magn Mater. 354 (2014) 340–344, https://doi.org/10.1016/j.jmmm.2013.11.008.
[8] S. Salman, S.S.S. Afghahi, M. Jafarian, Y. Atassi, Microstructural and magnetic studies on $BaMg_xZn_xX_{2x}Fe_{12-4x}O_{19}$ (X = Zr,Ce,Sn) prepared via mechanical activation method to act as a microwave absorber in X-band, J. Magn. Magn Mater. 406 (2016) 184–191, https://doi.org/10.1016/j.jmmm.2016.01.020.
[9] Z. Qiao, S. Pan, J. Xiong, L. Cheng, Q. Yao, P. Lin, Magnetic and microwave absorption properties of La-Nd-Fe alloys, J. Magn. Magn Mater. 423 (2017) 197–202, https://doi.org/10.1016/j.jmmm.2016.08.093.
[10] M. Bibi, S.M. Abbas, N. Ahmad, B. Muhammad, Z. Iqbal, U.A. Rana, S.U.D. Khan, Microwaves absorbing characteristics of metal ferrite/multiwall carbon nanotubes nanocomposites in X-band, Compos. B Eng. 114 (2017) 139–148, https://doi.org/10.1016/j.compositesb.2017.01.034.
[11] W. Widanarto, F.M. Rahayu, S.K. Ghoshal, M. Effendi, W.T. Cahyanto, Impact of ZnO substitution on magnetic response and microwave absorption capability of strontium-natural nanoferrites, Results Phys. 5 (2015) 253–256, https://doi.org/10.1016/j.rinp.2015.09.002.
[12] Y. Ma, Y. Zhou, Y. Sun, H. Chen, Z. Xiong, X. Li, L. Shen, Y. Liu, Tunable magnetic properties of Fe_3O_4/rGO/PANI nanocomposites for enhancing microwave absorption performance, J. Alloys Compd. 796 (2019) 120–130, https://doi.org/10.1016/j.jallcom.2019.04.310.
[13] Y. Huang, J. Ji, Y. Chen, X. Li, J. He, X. Cheng, S. He, Y. Liu, J. Liu, Broadband microwave absorption of Fe_3O_4 –$BaTiO_3$ composites enhanced by interfacial polarization and impedance matching, Compos. B Eng. 163 (2019) 598–605, https://doi.org/10.1016/j.compositesb.2019.01.008.
[14] W. Li, X. Qiao, M. Li, T. Liu, H.X. Peng, La and Co substituted M-type barium ferrites processed by sol-gel combustion synthesis, Mater. Res. Bull. 48 (2013) 4449–4453, https://doi.org/10.1016/j.materresbull.2013.07.044.
[15] Y. Liu, T.J. Wang, Y. Liu, X.J. Li, Y. Liu, Mechanism for synthesizing barium hexagonal ferrite by sol-gel method, Adv. Mater. Res. 549 (2012) 105–108 https://doi.org/10.4028/www.scientific.net/AMR.549.105.
[16] S. Bierlich, F. Gellersen, A. Jacob, J. Töpfer, Low-temperature sintering and magnetic properties of Sc- and In-substituted M-type hexagonal barium ferrites for microwave applications, Mater. Res. Bull. 86 (2017) 19–23, https://doi.org/10.1016/j.materresbull.2016.09.025.
[17] W. Jing, Z. Hong, B. Shuxin, C. Ke, Z. Changrui, Microwave absorbing properties of rare-earth elements substituted W-type barium ferrite, J. Magn. Magn Mater. 312 (2007) 310–313, https://doi.org/10.1016/j.jmmm.2006.10.612.
[18] G. Shen, Z. Xu, Y. Li, Absorbing properties and structural design of microwave absorbers based on W-type La-doped ferrite and carbon fiber composites, J. Magn. Magn Mater. 301 (2006) 325–330, https://doi.org/10.1016/j.jmmm.2005.07.007.
[19] W. Widanarto, F. Amirudin, S.K. Ghoshal, M. Effendi, W.T. Cahyanto, Structural and magnetic properties of La^{3+} substituted barium − natural nanoferrites as microwave absorber in X-band, J. Magn. Magn Mater. 426 (2017) 483–486, https://doi.org/10.1016/j.jmmm.2016.11.124.
[20] L. Deng, L. Ding, K. Zhou, S. Huang, Z. Hu, B. Yang, Electromagnetic properties and microwave absorption of W-type hexagonal ferrites doped with La^{3+}, J. Magn. Magn Mater. 323 (2011) 1895–1898, https://doi.org/10.1016/j.jmmm.2011.02.034.
[21] W. Widanarto, E. Ardenti, S.K. Ghoshal, C. Kurniawan, M. Effendi, W.T. Cahyanto, Significant reduction of saturation magnetization and microwave-reflection loss in barium-natural ferrite via Nd^{3+} substitution, J. Magn. Magn Mater. 456 (2018) 288–291, https://doi.org/10.1016/j.jmmm.2018.02.050.
[22] W. Widanarto, M. Jandra, S.K. Ghoshal, M. Effendi, W.T. Cahyanto, $BaCO_3$ mediated modifications in structural and magnetic properties of natural nanoferrites, J. Phys. Chem. Solid. 79 (2015) 78–81, https://doi.org/10.1016/j.jpcs.2014.12.011.
[23] V.S. Vinila, R. Jacob, A. Mony, H.G. Nair, S. Issac, S. Rajan, A.S. Nair, J. Isac, XRD studies on nano crystalline ceramic superconductor PbSrCaCuO at different treating temperatures, Cryst. Struct. Theor. Appl. (2014) 1–9, https://doi.org/10.4236/csta.2014.31001 03.
[24] S. Dabagh, A.A. Ati, R.M. Rosnan, S. Zare, Z. Othaman, Effect of Cu – Al substitution on the structural and magnetic properties of Co ferrites, Mater. Sci. Semicond. Process. 33 (2015) 1–8, https://doi.org/10.1016/j.mssp.2015.01.025.
[25] C.K. Das, P. Bhattacharya, S.S. Kalra, Graphene and MWCNT: potential candidate for microwave absorbing materials, J. Mater. Sci. Res. 1 (2012) 126, https://doi.org/10.5539/jmsr.v1n2p126.
[26] S. Kumar, R. Chatterjee, Complex permittivity , permeability , magnetic and microwave absorbing properties of Bi^{3+} substituted U-type hexaferrite, J. Magn. Magn Mater. 448 (2018) 88–93, https://doi.org/10.1016/j.jmmm.2017.06.123.
[27] K. Shi, J. Li, S. He, H. Bai, Y. Hong, Y. Wu, D. Jia, Z. Zhou, A superior microwave absorption material: Ni^{2+}-Zr^{4+} Co-Doped barium ferrite ceramics with large reflection loss and broad bandwidth, Curr. Appl. Phys. 19 (2019) 842–848, https://doi.org/10.1016/j.cap.2019.03.018.
[28] P. Meng, K. Xiong, L. Wang, S. Li, Y. Cheng, G. Xu, Tunable complex permeability and enhanced microwave absorption properties of $BaNi_xCo_{1-x}TiFe_{10}O_{19}$, J. Alloys Compd. 628 (2015) 75–80, https://doi.org/10.1016/j.jallcom.2014.10.163.
[29] J. Li, S. He, K. Shi, Y. Wu, H. Bai, Y. Hong, W. Wu, Q. Meng, Coexistence of broadbandwidth and strong microwave absorption, Ceram. Int. 44 (2018) 6953–6958, https://doi.org/10.1016/j.ceramint.2018.01.127.